

for the bpa-bridged dimer, k_1 ranges from 2.2×10^7 to 4.8×10^7 s⁻¹ over the temperature range 77–160 K.

Unfortunately, even at 77 K the intramolecular quenching event for the 4,4'-bpy-bridged dimer is too rapid to be seen with our time resolution (10 ns). In fact, our ability to observe the intramolecular electron-transfer event for the bpa-bridged dimer depends, in part, on the fact that the medium is a frozen matrix. Once the glass to fluid transition is reached, there is a marked decrease in lifetime, resulting in decay processes that are too rapid for our detection capabilities. A contribution to electron trapping arising from the orientation of surrounding solvent dipoles is certainly expected. By inference, a thermally activated component of this contribution may exist that begins to dominate electron transfer once the solvent dipoles become orientationally mobile.

Our observations reinforce those made earlier⁷ in suggesting a possible general approach to the problem of measuring intramolecular electron-transfer rate constants in mixed-valence dimers based on excitation of an appropriate chromophore within the dimer. Clearly in the systems chosen for study here, the intramolecular processes are sufficiently rapid that it will be necessary to apply picosecond techniques to the general problem of measuring the transient decays that occur after photolysis.

A final point of note is that the intramolecular process in eq 5 has the effect of creating a remote MLCT state where the excited electron and "hole" within the molecule have been separated by a ligand bridge. This is an important process in that it results in intramolecular charge separation and potentially in long-lived, intramolecular charge storage. However, a puzzling feature is that, once reached, the charge-separated state is relatively short-lived as shown by the k_3 values in Table II. We are currently investigating such states in more detail in order to understand the molecular mechanisms that lead to their rapid decay.

Acknowledgments are made to the National Science Foundation, Grant No. CHE-8008922, and to the Army Research Office, Durham, NC, Grant No. DAAG29-82-K-0111, for support of this research.

Registry No. [(bpy)₂(CO)Os^{II}(4,4'-bpy)Os^{II}(Cl)(phen)(dppe)][PF₆]₃, 96532-39-7; [(bpy)₂(CO)Os^{II}(bpa)Os^{II}(Cl)(phen)(dppe)][PF₆]₃, 96532-41-1; [(bpy)₂(CO)Os^{II}(4,4'-bpy)][PF₆]₂, 96503-61-6; [(phen)(Cl)Os^{II}(dppe)(4,4'-bpy)][PF₆]₂, 96503-63-8; [(bpy)₂(CO)Os^{II}(bpa)][PF₆]₂, 96503-65-0; [(phen)(Cl)Os^{II}(dppe)(bpa)][PF₆]₂, 96532-43-3.

Department of Chemistry
The University of North Carolina
Chapel Hill, North Carolina 27514

Kirk S. Schanze
Thomas J. Meyer*

Received August 9, 1984

EPR and Resonance Raman Studies of the (5,10,15,20-Tetraphenylporphinato)ferrate(I) Anion: Formation of a Five-Coordinate Pyridine Adduct

Sir:

The nature of highly reduced iron porphyrins is important because of their possible involvement as intermediates in the chemistry of cytochrome P-450 and peroxidases.²⁻⁵ In particular, whether the one-electron-reduction product of Fe(II) porphyrins is best described as an Fe(I) porphyrin or an Fe(II) porphyrin π anion radical (or a species intermediate between these two forms) remains unresolved.⁶ The EPR spectrum⁷ of [Fe(TPP)]⁻ is

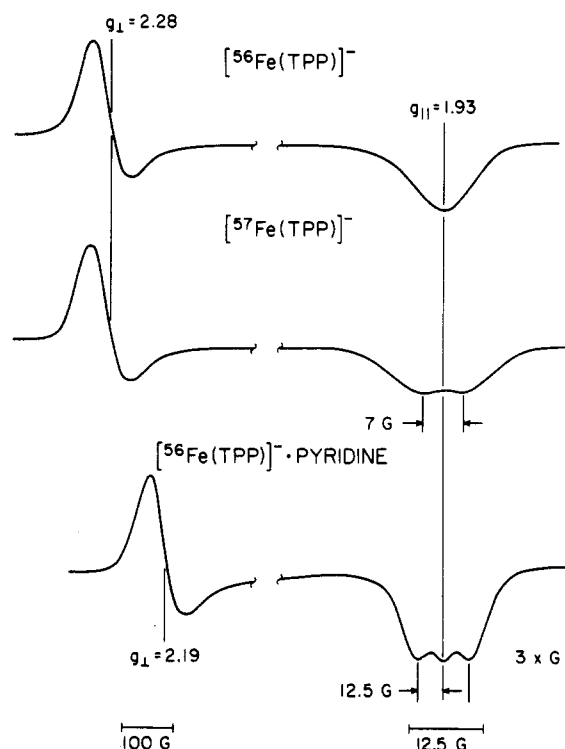


Figure 1. Low-temperature (77 K) X-band EPR spectra of DMF glasses of (top) [Fe(TPP)]⁻, (middle) [Fe(TPP)]⁻, and (bottom) [Fe(TPP)]⁻ plus 60 equiv of pyridine. Each sample was 2.0 mM. Conditions: microwave power 18.3 mW; modulation amplitude 2 G.

characteristic of an axially symmetric spin system with $g_{\perp} = 2.28$ and $g_{\parallel} = 1.93$ and, by comparison with low-spin d⁷ Co(II) porphyrins, has been the basis for a low-spin Fe(I) formulation.⁸⁻¹⁰ A recent deuterium NMR study supports the Fe(I) formulation.¹¹ On the other hand, [Fe(TPP)]⁻ exhibits an unusual optical spectrum that includes a low-intensity split Soret band and a five-banded visible region,^{6,12} which may indicate the presence of substantial electron density on the porphyrin ring. The anion radical formulation is further supported by crystallographic data for [Na(DB-18-crown-6)(THF)₂]⁺[Fe(TPP)]⁻, which shows that the Fe-N_{pyrrole} bond lengths of [Fe(TPP)]⁻ are shorter than those of Fe(TPP).¹³

As a means to resolve the electronic nature of the [Fe(TPP)]⁻ species, the EPR spectra have been recorded for the ⁵⁷Fe-substituted complex and for the ⁵⁶Fe species in the presence of potential axial ligands (pyridine and *N*-MeIm). Resonance Raman spectra of the [Fe(TPP)]⁻ complex have also been measured.

Figure 1 illustrates the low-temperature (77 K) EPR spectra of [Fe(TPP)]⁻, [Fe(TPP)]⁻, and [Fe(TPP)]⁻ in the presence of pyridine.^{14,15} The g_{\parallel} signal of [Fe(TPP)]⁻ is split into a poorly

- (1) Alfred P. Sloan Foundation Fellow, 1982–1986.
- (2) Collman, J. P.; Sorrell, T. N.; Dawson, J. H.; Trudel, R. J.; Bunnenberg, E.; Djerassi, C. *Proc. Natl. Acad. Sci. U.S.A.* **1976**, *73*, 6–10.
- (3) Reed, C. A.; Mashiko, T.; Scheidt, W. R.; Haller, K. 1st International Symposium on O₂ Activation and Selective Oxidations Catalyzed by Transition Metals, Bendor, France, 1979; Poster abstract.
- (4) Welborn, C. H.; Dolphin, D.; James, B. R. *J. Am. Chem. Soc.* **1981**, *103*, 2869–2871.
- (5) Lexa, D.; Savaent, J.-M. *J. Am. Chem. Soc.* **1982**, *104*, 3503–3504.
- (6) For a review of this point see: Reed, C. A. *Adv. Chem. Ser.* **1982**, 333–356.

- (7) Abbreviations: EPR, electron paramagnetic resonance; NMR, nuclear magnetic resonance; Fe(TPP), Fe(II) tetraphenylporphyrin; DB-18-crown-6, dibenzo-18-crown-6; DMF, dimethylformamide; Me₂SO, dimethyl sulfoxide; *N*-MeIm, *N*-methylimidazole.
- (8) Cohen, I. A.; Ostfeld, D.; Lichenstein, B. *J. Am. Chem. Soc.* **1972**, *94*, 4522–4525.
- (9) Lexa, D.; Momenteau, M.; Mispelter, J. *Biochim. Biophys. Acta* **1974**, *338*, 151–153.
- (10) Kadish, K. M.; Larson, G.; Lexa, D.; Momenteau, M. *J. Am. Chem. Soc.* **1975**, *97*, 282–288.
- (11) Hickman, D. L.; Shirazi, A.; Goff, H. M. *Inorg. Chem.* **1985**, *24*, 563–566.
- (12) Jones, S. E.; Srivatsa, G. S.; Sawyer, D. T.; Traylor, T. G.; Mincey, T. C. *Inorg. Chem.* **1983**, *22*, 3903–3910.
- (13) Mashiko, T.; Reed, C. A.; Haller, K. J.; Scheidt, W. R. *Inorg. Chem.* **1984**, *23*, 3192–3196.
- (14) ⁵⁷Fe(II)(TPP)Cl was synthesized by a modified procedure of: Burke, J. M.; Kincaid, J. R.; Spiro, T. G. *J. Am. Chem. Soc.* **1978**, *100*, 6077–6083. ⁵⁷Fe was obtained as ⁵⁷Fe₂O₃ (90.24% enriched) from Oak Ridge National Laboratories. TPP was purchased from Midcentury (Posen, IL). Fe(TPP) and [Fe(TPP)]⁻ were generated electrochemically in an inert-atmosphere box as described in ref 12.

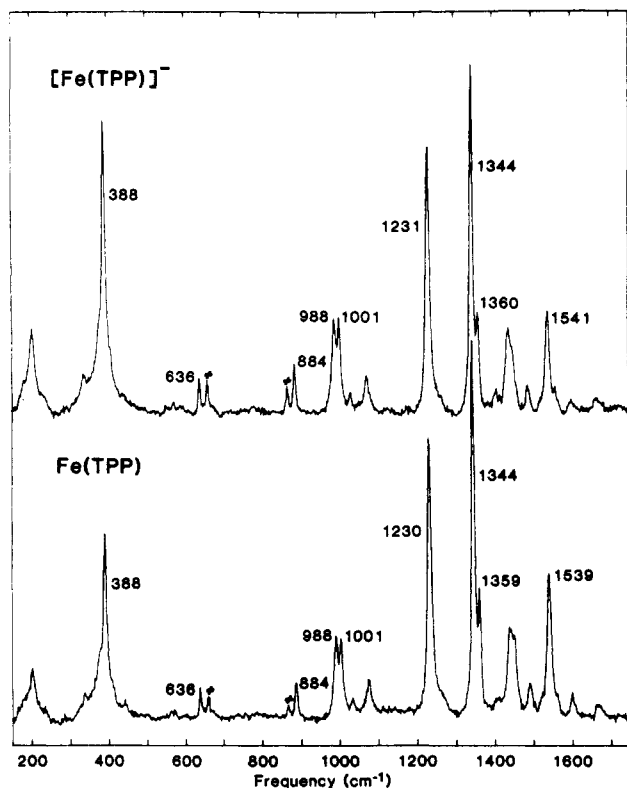


Figure 2. Room-temperature Soret excitation Resonance Raman spectra of (top) 0.25 mM $[\text{Fe}(\text{TPP})]^-$ and (bottom) 0.25 mM $\text{Fe}(\text{TPP})$ in DMF. Solvent peaks are labeled by #. Conditions: $\lambda_{\text{ex}} = 4131 \text{ \AA}$, laser power 20 mW; spectral resolution 3 cm^{-1} .

resolved doublet due to ^{57}Fe hyperfine interactions ($A_{\parallel}^{57\text{Fe}} \sim 7.0 \text{ G}$, 18.9 MHz), while no hyperfine structure is observed in the g_{\perp} region. In the presence of pyridine, the $[\text{Fe}(\text{TPP})]^-$ complex yields EPR signals at $g_{\perp} = 2.19$ and $g_{\parallel} = 1.93$, as has been reported previously.⁸ However, contrary to earlier studies, superhyperfine structure is clearly evident in the g_{\parallel} region due to electron interactions with the ^{14}N nucleus ($A_{\parallel}^{14\text{N}} \sim 12.5 \text{ G}$, 33.8 MHz) of a single axial pyridine ligand. Analogous splitting or broadening is not observed in the g_{\perp} region. (Similar results are obtained upon addition of *N*-MeIm.) These spectra represent the first *definitive* evidence for axial ligation to $[\text{Fe}(\text{TPP})]^-$. The general appearance of the ^{57}Fe and ^{14}N hyperfine pattern (large in the g_{\parallel} region and small in the g_{\perp} region) parallels the metal and axial ligand hyperfine pattern observed for $d^7 \text{Co(II)}$ porphyrins.¹⁶ In addition, the magnitude of $A_{\parallel}^{14\text{N}}$ observed for $[\text{Fe}(\text{TPP})](\text{py})^-$ is nearly identical with that observed for the pyridine adduct of Co(II) porphyrins¹⁶ and Fe(I) phthalocyanine.¹⁷ These results are consistent only with an Fe(I) formulation for $[\text{Fe}(\text{TPP})]^-$.

Resonance Raman spectra have been reported for a number of one-electron-reduced metal(II) porphyrins, including $[\text{Zn}(\text{T-PP})]^-$ and $[\text{Mg}(\text{TPP})]^-$.¹⁸⁻²⁰ The latter two species are clearly porphyrin π anion radicals and exhibit certain skeletal vibrational frequencies that differ by as much as 20 cm^{-1} from those of their oxidized counterparts.²⁰ The room-temperature resonance Raman spectra of $\text{Fe}(\text{TPP})$ and $[\text{Fe}(\text{TPP})]^-$ are compared in Figure 2.^{21a} As can be seen, the frequencies of analogous vibrational modes of the two complexes are identical to within 2 cm^{-1} . On the other

hand, the relative resonance-enhanced Raman intensities for analogous modes are somewhat different (compare the intensities of the 388 - and 1344-cm^{-1} bands),^{21b} as is expected because the Soret absorption maxima are different for the two species.^{6,12} The similarity of the skeletal frequencies for $\text{Fe}(\text{TPP})$ and $[\text{Fe}(\text{TPP})]^-$ is incompatible with substantial porphyrin π -anion-radical character for the reduced complex. The spectral similarities between the $d^7 \text{Fe(I)}$ and $d^6 \text{Fe(II)}$ porphyrins, however, are consistent with observations made for the isoelectronic Co(II) and Co(III) systems.^{22,23}

Neither the resonance Raman spectrum nor the optical spectrum of $[\text{Fe}(\text{TPP})]^-$ obtained at room temperature is altered by the addition of pyridine. The resonance Raman data probably cannot be regarded as conclusive, because the skeletal frequencies of $d^7 \text{Co(II)}$ porphyrins are known to be relatively insensitive to the presence of axial nitrogen bases.²² On the other hand, the absence of change in the optical spectrum upon pyridine addition strongly suggests that axial ligation does not occur at room temperature.²⁴

In summary, the EPR and resonance Raman spectra for $[\text{Fe}(\text{TPP})]^-$ support a $d^7 \text{Fe(I)}$ formulation for the complex (both at low temperature and room temperature.) These data argue against a resonance formulation in which there is a substantial admixture of anion-radical character into the ground-state wave function.^{6,25} Such an admixture should result in hyperfine values and vibrational frequencies between those expected for the two limiting cases and commensurate with the percentage contribution of each species. This is not observed. The EPR data also confirm that $[\text{Fe}(\text{TPP})]^-$ can bind a single axial ligand, at least in frozen solutions. Finally, the Fe(I) formulation is consistent with the electrochemical behavior of $\text{Fe}(\text{TPP})$. The reduction potential for $\text{Fe}(\text{TPP})$ in Me_2SO or DMF is 150 mV less negative than that for $\text{Zn}(\text{TPP})$.¹² If the addition of an electron to $\text{Fe}(\text{TPP})$ resulted in the formation of an anion radical (as is the case for $\text{Zn}(\text{TPP})$),

- (21) (a) Resonance Raman spectra of samples sealed in capillary tubes were obtained by the use of various excitation lines from Kr and Ar ion lasers. The spectrometer has been described: Schick, G. A.; Bocian, D. F. *J. Am. Chem. Soc.* **1983**, *105*, 1830-1838. The integrity of the $[\text{Fe}(\text{TPP})]^-$ sample and, in particular, its stability to photooxidation to $\text{Fe}(\text{TPP})$ were monitored by recording both the optical spectrum and the Raman spectrum before, during, and after laser irradiation. The sample was contained in a tightly sealed optical microcell equipped with a capillary sidearm that served as the Raman cell. The entire volume monitored in the optical experiment could be contained in the capillary portion of the cell. To ensure that all of the sample in the capillary was irradiated, the laser beam was moved down the length of the 8-mm tube in eight steps of 1 mm each. At each point, the sample was irradiated for 30 min (the entire period of a Raman experiment) at 4 times the power level used in the Raman experiment. At no time during or after irradiation was the Raman or optical spectrum altered from that consistent with $[\text{Fe}(\text{TPP})]^-$. (b) Resonance Raman spectra were recorded for both $\text{Fe}(\text{TPP})$ and $[\text{Fe}(\text{TPP})]^-$ at several different excitation wavelengths in the violet region of the spectrum. The ratios of the Raman intensities, $I(\lambda_{\text{ex}} = 4131 \text{ \AA})/I(\lambda_{\text{ex}} = 4067 \text{ \AA})$, for the 388 -, 1231 -, 1344 -, and 1540-cm^{-1} bands were observed to be for $\text{Fe}(\text{TPP})$ [2.5, 2.1, 4.7, 4.7] and for $[\text{Fe}(\text{TPP})]^-$ [1.6, 2.8, 2.7, 2.5]. The large increase in the intensity of Raman scattering observed for $\text{Fe}(\text{TPP})$ as the excitation wavelength is moved to the red is expected because this complex has a very strong absorption maximum near 424 nm .⁶ Similarly, the much smaller increase in Raman intensity observed for $[\text{Fe}(\text{TPP})]^-$ is consistent with the moderate increase in absorption intensity between $\lambda_{\text{ex}} = 4067$ and 4131 \AA . The different nature of the scattering species is also reflected in very different intensity ratios of *different* bands of the *same* species as the excitation wavelength is varied.

- (22) Woodruff, W. H.; Adams, D. H.; Spiro, T. G.; Yonetani, T. *J. Am. Chem. Soc.* **1975**, *97*, 1695-1698.

- (23) Spaulding, L. D.; Chang, C. C.; Yu, N.-T.; Felton, R. H. *J. Am. Chem. Soc.* **1975**, *97*, 2517-2525.

- (24) Stynes, D. V.; Stynes, H. C.; James, B. R.; Ibers, J. A. *J. Am. Chem. Soc.* **1973**, *95*, 1796-1801.

- (25) The observation that $[\text{Fe}(\text{TPP})]^-$ is best formulated as an Fe(I) species does not invalidate the resonance concept. EPR studies by Kadish and co-workers (Kadish, K. M.; Boisselier-Cocolios, B.; Simonet, B.; Chang, D.; Ledon, H.; Cocolios, P. *Inorg. Chem.*, in press) indicate that reduction of pyrrole-substituted tetracyano- Fe(II) -TPP complexes results in a species exhibiting all g values between 2.03 and 1.98. This system clearly contains π -anion-radical character and is best described in terms of the resonance formulation advanced in ref 6. Thus, it appears that the exact nature of the reduced species strongly depends on the type of porphyrin ligand.

(15) EPR spectra were recorded on a Bruker ER-200D X-band spectrometer by use of a liquid- N_2 finger Dewar.

(16) Walker, F. A. *J. Am. Chem. Soc.* **1970**, *92*, 4235-4244.

(17) Lever, A. B. P.; Wilshire, J. P. *Inorg. Chem.* **1978**, *17*, 1145-1151.

(18) Spiro, T. G. In "Iron Porphyrins"; Lever, A. B. P., Gray, H. B., Eds.; Addison-Wesley: Reading, MA, 1983; Vol. II; pp 89-152.

(19) Ksenofontova, N. M.; Maslov, V. G.; Sidorov, A. N.; Bobovich, Y. S. *Opt. Spectrosc.* **1976**, *40*, 462-465.

(20) Yamaguchi, H.; Soeta, A.; Toeda, H. *J. Electroanal. Chem.* **1983**, *159*, 347-359.

then the reduction potentials would be expected to be essentially the same. The enhanced ease of electron addition must be due to the unfilled d subshells of Fe(II).

Our results are partially at variance with the crystallographic data reported for $[\text{Na}(\text{DB-18-crown-6})(\text{THF})_2]^+[\text{Fe}(\text{TPP})]^-$.¹³ The latter complex, which was crystallized from a pyridine solution, does not give any evidence for axial ligation and has a different skeletal geometry from Fe(TPP). Indeed, our optical studies indicate that axial ligation apparently occurs only at low temperatures in frozen solutions. On the other hand, geometry differences of the reported magnitude should result in observable vibrational frequency differences.¹⁸ Solid-state effects might be the origin of the geometric differences between crystalline Fe(TPP) and $[\text{Fe}(\text{TPP})]^-$, since the present Raman studies do not indicate that there are substantial differences for the solution species at room temperature. Nevertheless, the explanation for the unusual optical spectrum of $[\text{Fe}(\text{TPP})]^-$ remains unclear and must await a rigorous theoretical investigation.

Acknowledgment. We thank Dr. Hiroshi Sugimoto for assistance with the synthesis of $^{57}\text{Fe}(\text{TPP})\text{Cl}$ and Professor Harold M. Goff for providing a preprint of the manuscript describing his deuterium NMR study. This work was supported by the National Science Foundation, under Grant No. CHE-8212299 (D.T.S.), and the National Institutes of Health, under Grant No. GM-30078 (D.F.B.).

Registry No. $[\text{Fe}(\text{TPP})]^-$, 54547-68-1; $[\text{Fe}(\text{TPP})(\text{py})]^-$, 96531-99-6; Fe(TPP), 16591-56-3.

Department of Chemistry
University of California
Riverside, California 92521

G. Susan Srivatsa
Donald T. Sawyer
Nancy J. Boldt
David F. Bocian*¹

Received November 14, 1984

Solution Structure of Five-Coordinate Complexes of Ruthenium(II): Evidence for a Square-Pyramidal Geometry for the Cations $[\text{RuXL}_4]^+$ (X = H, C_2Ph ; L = PMe_2Ph)

Sir:

We wish to report 32-MHz $^{31}\text{P}\{^1\text{H}\}$ NMR studies of the five-coordinate cations $[\text{RuXL}_4]^+$ (X = H, C_2Ph ; L = PMe_2Ph), which, in conjunction with corresponding data from the closely related six-coordinate species $[\text{RuX}(\text{PMe}_2(\text{MeO}-2-\text{C}_6\text{H}_4))_4]^+$, provide the first direct evidence of the square-pyramidal geometry in solution for five-coordinate d^6 metal complexes containing phosphine ligands.

Although X-ray diffraction studies¹ and a theoretical treatment² indicate that the square pyramid is the more favored geometry for five-coordinate d^6 ions, experimental evidence for this structure in solution has proved elusive. For example, the catalytically important complexes $[\text{RuCl}_2(\text{PPh}_3)_3]$ ³ and $[\text{RuHCl}(\text{PPh}_3)_3]$ ⁴ in the solid state are square-pyramidal^{5,6} but in solution at low temperature show an A_2X pattern of $^{31}\text{P}\{^1\text{H}\}$ signals¹ and cannot therefore rule out the alternative trigonal-bipyramidal structure. In complexes with four coordinated phosphorus nuclei, distinction

Table I. ^{31}P NMR Data for $[\text{RuXL}_4][\text{PF}_6]$ Complexes

L	X	T^a	δ_A^b	δ_M^b	δ_X^b	J_{AM}^c	J_{AX}	J_{MX}
PMe_2Ph	$\text{C}\equiv\text{CPh}$	183	4.7	-3.1	30.4	26	33	26
$\text{PMe}_2(\text{oA})^d$	$\text{C}\equiv\text{CPh}$	303	-0.5	6.2	28.2	33	28	33
PMe_2Ph	H	193	9.2	-8.2	33.8	20	37	20
$\text{PMe}_2(\text{oA})$	H	273	4.5 ^e		38.2		38	20

^a Temperature in kelvins. ^b Chemical shifts relative to external H_3PO_4 . ^c Coupling constants in hertz. ^d oA = $\text{MeO}-2-\text{C}_6\text{H}_4$. ^e Second-order system not analyzed.

between the two stereochemistries by ^{31}P NMR should be straightforward, the square-pyramidal geometry giving A_2MX or A_4 spectra and the trigonal-bipyramidal A_2X_2 or A_3X spectra. Thus, McAuliffe et al. have interpreted⁷ the ^{31}P NMR spectra of $[\text{RuX}(\text{L}_2)_2][\text{BPh}_4]$ ($\text{L}_2 = \text{Ph}_2\text{P}(\text{CH}_2)_3\text{PPh}_2$, X = Cl; $\text{L}_2 = \text{Ph}_2\text{P}(\text{CH}_2)_3\text{PMe}_2$, X = H, Cl) as showing a rigid trigonal-bipyramidal structure for these complexes. Their observations do not, however, constitute "unambiguous findings", as claimed (vide infra).

The salt $[\text{Ru}(\text{C}\equiv\text{CPh})\text{L}_4][\text{PF}_6]$ (**1**; L = PMe_2Ph),^{8a} prepared from $[\text{RuHL}_5][\text{PF}_6]$ ⁹ and $\text{PhC}\equiv\text{CH}$, shows a single ^{31}P resonance (15 ppm) at 30 °C in CD_2Cl_2 which at -60 °C separates into three signals of intensity 1:2:1 ($\text{X}:\text{A}_2:\text{M}$) and at -90 °C resolves into three multiplets characterized by the parameters in Table I. The line widths of ~6 Hz prevent distinction between the values of J_{AM} and J_{MX} . The color of the solution at all temperatures is the same as observed in the solid state, viz. purple, which discounts the possibility of strong solvation.^{8b}

The NMR pattern is clear evidence^{8c} in favor of the square-pyramidal geometry for this complex and the substantial deshielding of the signal assigned as the apical phosphorus P_X is reminiscent of the data for $[\text{RuCl}_2(\text{PPh}_3)_3]$ and $[\text{RuHCl}(\text{PPh}_3)_3]$ in which the great difference in ^{31}P chemical shifts suggests that the square-pyramidal structure is maintained as it is characterized by widely different bond lengths $\text{Ru}-\text{P}_{\text{basal}} > \text{Ru}-\text{P}_{\text{apical}}$.^{5,6} The crystal structure determination⁸ of complex **1** gives the metal-phosphorus bond lengths $\text{Ru}-\text{P}_A = 2.40 \text{ \AA}$, $\text{Ru}-\text{P}_M = 2.34 \text{ \AA}$, and $\text{Ru}-\text{P}_X = 2.22 \text{ \AA}$, reaffirming the correlation with $\delta(^{31}\text{P})$ values.

The room-temperature ^{31}P spectrum of complex **1** [L = $\text{PMe}_2(\text{MeO}-2-\text{C}_6\text{H}_4)$] is also of the A_2MX type, but in this case an OMe group is weakly coordinated¹¹ cis to the alkynyl ligand, thus generating a pseudooctahedral geometry.

The hydride complexes show changes with temperature similar to those of their alkynyl analogues; the solution in CD_2Cl_2 of six-coordinate $[\text{RuHL}_4]^+$ [**2**; L = $\text{PMe}_2(\text{MeO}-2-\text{C}_6\text{H}_4)$], which has a structure¹¹ analogous to the corresponding alkynyl complex,

(7) Briggs, J. C.; McAuliffe, C. A.; Dyer, G. J. *Chem. Soc., Dalton Trans.* **1984**, 423.

(8) (a) Ashworth, T. V.; Kruger, G. J.; Singleton, E., unpublished results. ^1H NMR showed samples did not contain solvent of crystallization (e.g. ethanol), which might have affected the ^{31}P NMR results. (b) In acetone solution, however, the complex is colorless at -50 °C showing solvation. (c) A reviewer has suggested the possibility that the observed pattern may arise from a trigonal-bipyramidal structure in which restricted rotation about the metal-phosphorus bonds gives rise to rotamers. We do not consider this a viable alternative since such a structure would render all phosphorus atoms nonequivalent and give rise to very different coupling constants. In addition, the salt $[\text{RuH}(\text{Ph}_2\text{P}(\text{CH}_2)_4\text{PPh}_2)_2][\text{PF}_6]$,¹⁰ in which the use of bidentate ligands precludes rotamer complications, also gives rise to an A_2MX ^{31}P pattern (acetone- d_6 , -80 °C): δ 78.6 (t), 37.9 (dd), -14.7 (t); $J_{AM} = 21$, $J_{AX} = 30$, $J_{MX} \leq 6$ Hz (M, X signals broadened); color of solution dark red.

(9) Ashworth, T. V.; Laing, M.; Nolte, M. J.; Singleton, E. *J. Chem. Soc., Dalton Trans.* **1977**, 1816.

(10) Ashworth, T. V.; Singleton, E. *J. Chem. Soc., Chem. Commun.* **1976**, 705.

(11) The X-ray crystal structures of both **1** and **2** [L = $\text{PMe}_2(\text{MeO}-2-\text{C}_6\text{H}_4)$] have been determined,¹² and the Ru-O distances of the coordinated methoxy group are 2.33 (3) and 2.31 (4) Å, respectively. This indicates weak bonding.¹³ That the Ru-O interaction is maintained in solution is shown by the downfield shift of a methoxy carbon atom in the ^{13}C NMR spectrum of each of the compounds.¹⁴

(12) Ashworth, T. V.; Levendis, D. C.; Singleton, E., unpublished results.

(13) Jeffrey, J. C.; Rauchfuss, T. B. *Inorg. Chem.* **1979**, *18*, 2658.

(14) Roundhill, D. M.; Roundhill, S. G. N.; Beaulieu, W. B.; Baghi, U. *Inorg. Chem.* **1980**, *19*, 3365.

(1) Hoffman, P. R.; Caulton, K. G. *J. Am. Chem. Soc.* **1975**, *97*, 4221.

(2) Pearson, R. G. *J. Am. Chem. Soc.* **1969**, *91*, 4947.

(3) Stephenson, T. A.; Wilkinson, G. *J. Inorg. Nucl. Chem.* **1966**, *28*, 945.

(4) Hallman, P. S.; McGarvey, B. R.; Wilkinson, G. *J. Chem. Soc. A* **1968**, 3143.

(5) La Placa, S. J.; Ibers, J. A. *Inorg. Chem.* **1965**, *4*, 778.

(6) Skapski, A. C.; Troughton, P. G. *H. J. Chem. Soc., Chem. Commun.* **1968**, 1230.